Electronic Supplementary Material (ESI) for Nanoscale.
This journal is © The Royal Society of Chemistry 2019

Towards low-loss telecom-wavelength photonic devices by designing $GaBi_xAs_{1-x}$/GaAs core−shell nanowires

Muhammad Usman[1,*]

[1] *School of Physics, The University of Melbourne, Parkville, 3010, Victoria, Australia.*

Supplementary Information Document

COMPUTATIONAL METHODS

Geometry Parameters: The schematic diagram of the investigated $GaBi_xAs_{1-x}$/GaAs nanowire is shown in the Figure 1(a) of the main text. In our study, the core−shell nanowires consist of a $GaBi_xAs_{1-x}$ core region with diameter D_C, length L, and Bi fraction x. The shell region is made up of GaAs material with diameter D_S and length L. The largest nanowire with D_S=30 nm and L=80 nm consists of about 3.5 million atoms and the smallest nanowire with D_S=10 nm and L=80 nm consists of about 0.37 million atoms. The simulations over large structures with atomistic resolution and realistic boundary conditions allow us to provide a highly reliable theoretical analysis of the nanowire electronic and optical properties.

In our simulations, the Bi atoms are randomly placed replacing the As atoms in the core region of the nanowires. The random spatial distribution of the Bi atoms is dependent on a four-digit seed value input to a random number generator that determines the nature of an anion atom (either Bi or As) at a given atomic location inside the nanowire core region. Different seed values ensure different spatial arrangements of the Bi atoms, resulting in statistically different numbers and types of Bi pairs and clusters in the core region. All of the results presented in this study are based on an average over five different random distributions of the Bi atoms.

It is critically important to simulate a large size for the $GaBi_xAs_{1-x}$ supercell to properly model the alloy disorder effects [1]. In our previous study on quantum well structures, We have probed the electron and hole energies as well as the associated inhomogeneous broadening in the ground state transition energies when the strained $GaBi_xAs_{1-x}$ supercell size is increased from 1000 atoms to 512000 atoms[2]. Our calculations showed that the small size of supercells (< 4096 atoms) artificially modifies the electron/hole energies and enhance the strength of the inhomogeneous broadening. By increasing the supercell size from 8000 atoms to 512000 atoms, we found that the electron and hole energies changed by less than 1 meV and 10 meV respectively, whereas the values of the inhomogeneous broadening for the hole energies were roughly 27 meV in good agreement with the measured value of 31 meV[1]. We therefore believe that a supercell size consisting of 8000 atoms or more is suitable to provide a reliable estimate of the properties of the strained $GaBi_xAs_{1-x}$ alloys. In this work on nanowires, we have performed large-scale atomistic simulations consisting of up to 3.5 million atoms in the over supercell, including the number of atoms in the $GaBi_xAs_{1-x}$ core region above 50000 in all cases.

Calculation of Strain: In order to calculate the strain induced by the lattice-mismatch between the GaAs and $GaBi_xAs_{1-x}$ materials, the $GaBi_xAs_{1-x}$/GaAs nanowires are relaxed by applying atomistic valence force field (VFF) energy minimization scheme[3–5]. The VFF parameters for the GaBi and GaAs materials are

published in the literature[5]. The values of α_0 and β_0 for the GaAs are taken from Lazarenkova *et al.*[4], whereas for GaBi are determined by obtaining relaxed bond lengths in accordance with Kent *et al.*[6].

After the VFF relaxation, the relaxed Ga-Bi bond-lengths are found to follow the trends of x-ray absorption spectroscopy measurements[5]. The strain tensor components ($\epsilon_{xx}, \epsilon_{yy}, \epsilon_{zz}, \epsilon_{xy}, \epsilon_{yz}, \epsilon_{xz}$) are computed from the relaxed bond-lengths of atoms[4]. The strain parameters of interest, which are directly related to the energy shifts in the conduction and valence band edges are hydrostatic (ϵ_H) and biaxial (ϵ_B) strain components, which are defined as follows[7]:

$$\epsilon_{\mathrm{H}} = \epsilon_{xx} + \epsilon_{yy} + \epsilon_{zz} \tag{1}$$

$$\epsilon_{\mathrm{B}} = 2\epsilon_{zz} - \epsilon_{xx} + \epsilon_{yy} \tag{2}$$

Electronic and Optical Simulations: The electronic structure of the studied nanowires is computed from the nearest-neighbour ten-band sp^3s^* tight-binding (TB) theory, which explicitly include spin-orbit coupling. The TB parameters for the GaAs and GaBi materials were published in our previous study[5], which accurately reproduced the bulk band structure of these two materials computed from DFT model[8]. In the published studies on both unstrained and strained $\mathrm{GaBi}_x\mathrm{As}_{1-x}$ alloys, the tight-binding model has shown good agreement with a series of available experimental data sets[1,5,9–14], as well as with the DFT calculations reported in the literature[15–17].

By solving the tight-binding Hamiltonian, we obtain ground state electron and hole energies and the corresponding wave functions at the Γ point (k=0), which are labelled as $|\psi_e\rangle$ and $|\psi_h\rangle$, respectively, and are defined as:

$$|\psi_e\rangle = \sum_{i,\mu} C^e_{i,\mu} |i\mu\rangle \tag{3}$$

$$|\psi_h\rangle = \sum_{j,\nu} C^h_{j,\nu} |j\nu\rangle \tag{4}$$

where the label i (j) represents the atom number inside the supercell and μ (ν) denotes the orbital basis states on an atom for the electron (hole) states. $C^e_{i,\mu}$ and $C^h_{j,\nu}$ are the coefficients of the electron and hole wave functions, respectively, computed by diagonalising the TB Hamiltonian.

The overlap between the electron and hole ground states is computed as follows:

$$|\langle\psi_h|\psi_e\rangle| = |\sum_{i=j}\sum_{\mu=\nu}(C^h_{j,\nu})^* C^e_{i,\mu}| \tag{5}$$

The inter-band optical transition strength between the ground electron and hole states is computed by

first computing the momentum matrix element as follows[7]:

$$M_{\overrightarrow{n}}^{\alpha\beta} = \sum_{i,j} \sum_{\mu,\nu} (C_{i,\mu,\alpha}^{e})^{*} (C_{j,\nu,\beta}^{h}) \langle i\mu\alpha|\mathbf{H}|j\nu\beta\rangle (\overrightarrow{n}_i - \overrightarrow{n}_j) \tag{6}$$

where α and β represent spin of states, $\mathbf{H}$ is the sp^3s^* tight-binding Hamiltonian, and $\overrightarrow{n} = \overrightarrow{n}_i - \overrightarrow{n}_j$ is the real space displacement vector between atoms i and j, and is equal to $\overrightarrow{x}_i - \overrightarrow{x}_j$. The optical transition strengths is then calculated by using the Fermi's Golden rule and summing the absolute values of the momentum matrix elements over the spin degenerate states:

$$\text{Optical Absorption} = \sum_{\alpha,\beta} |M_{\overrightarrow{x}}^{\alpha\beta}|^2 \tag{7}$$

The tight-binding model is implemented with in the framework of atomistic tool NanoElectronic Modeling (NEMO 3-D) simulator[18] which has, in the past, shown an unprecedented accuracy to match experiments for the study of nano-materials[1,5,19] and devices[7,20].

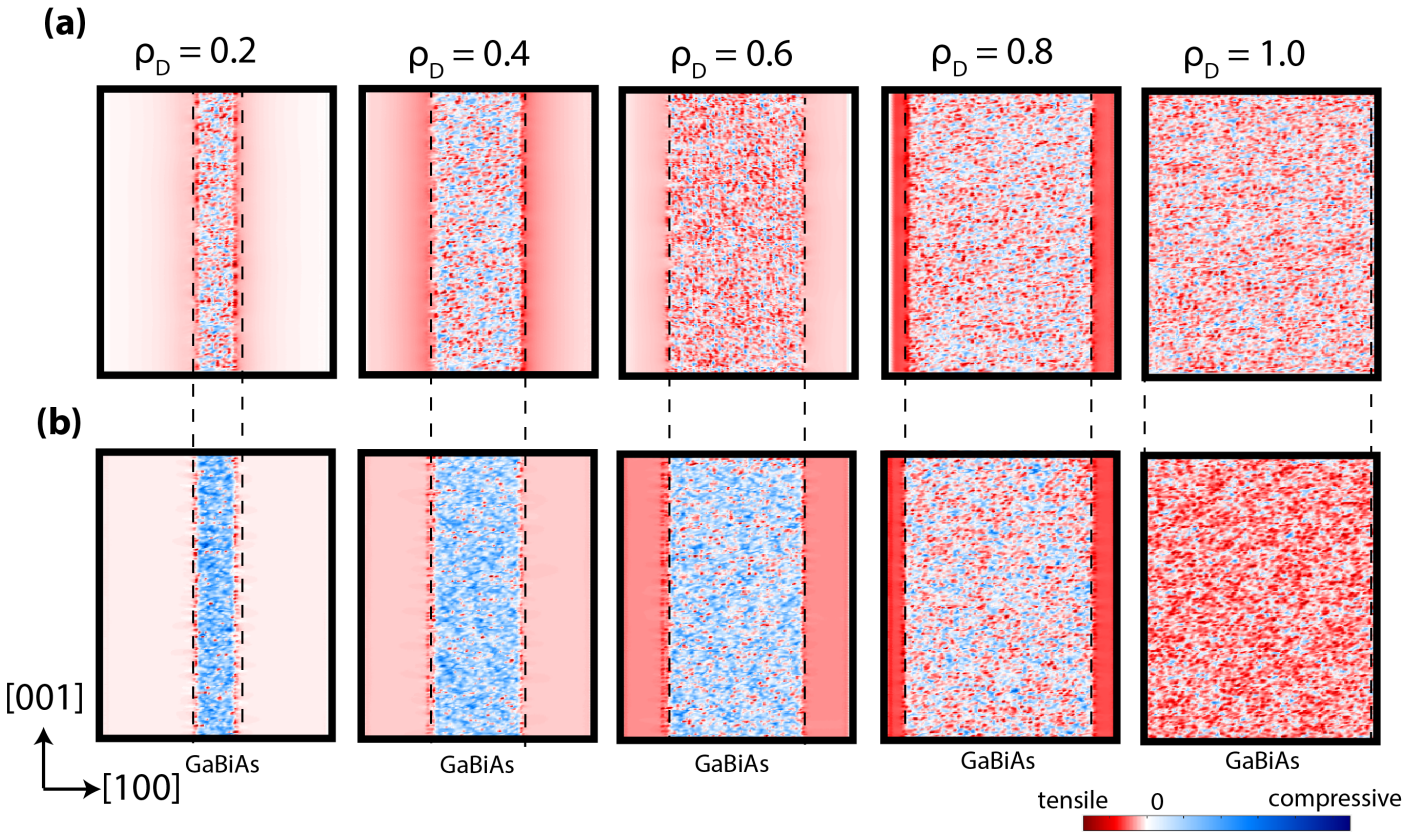

Supplementary Fig. S1. **(a)** The plots of strain tensor component (ϵ_{xx}) are shown for the $GaBi_xAs_{1-x}$/GaAs nanowire with x=15%, ρ_L=4, a few selected values of ρ_D. The color plots show the strain profile in a 2D plane through the center of the nanowire. The blue (red) color regions indicate the presence of compressive (tensile) strain. **(b)** The same as **(a)** but for the strain tensor component (ϵ_{zz}).

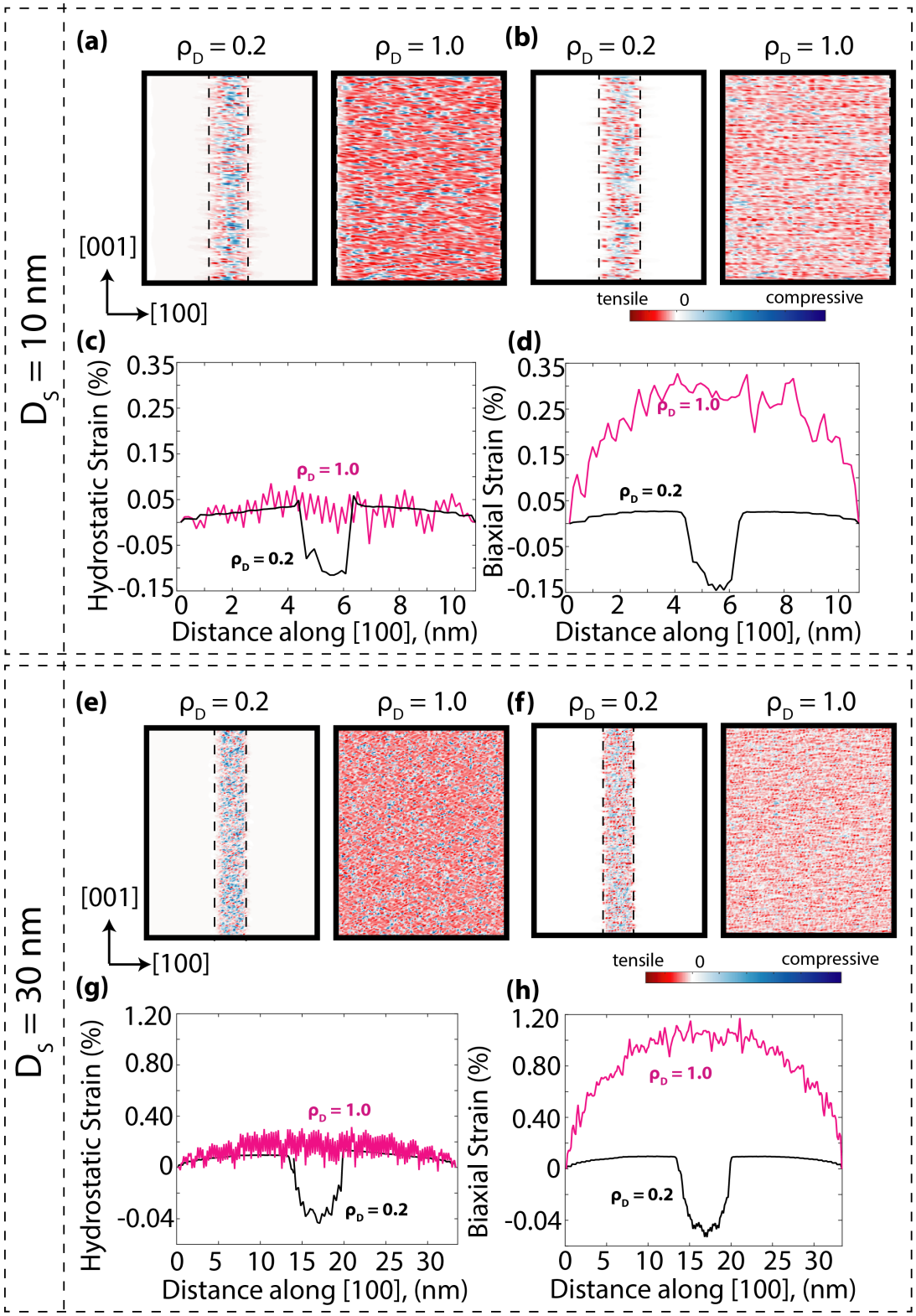

Supplementary Fig. S2. **(a,b)** The plots of the hydrostatic and biaxial strain components are shown for the nanowire structure with x=15%, D_S=10 nm, ρ_L=8, a couple of selected values of ρ_D. The color plots show the strain profiles in a 2D [010]-plane through the center of the nanowires. The blue (red) color regions indicate the presence of a compressive (tensile) strain. **(c,d)** The 1D plots of the hydrostatic and biaxial strain components are shown through the center of the nanowire. The computed strain at each data point along the [100] direction represents an average over all data points in the corresponding [100] plane and for five different random configurations of Bi atoms. **(e-h)** The same as **(a-d)** but for the nanowire structures with x=15%, D_S=30 nm, ρ_L=2.67, a couple of selected values of ρ_D.

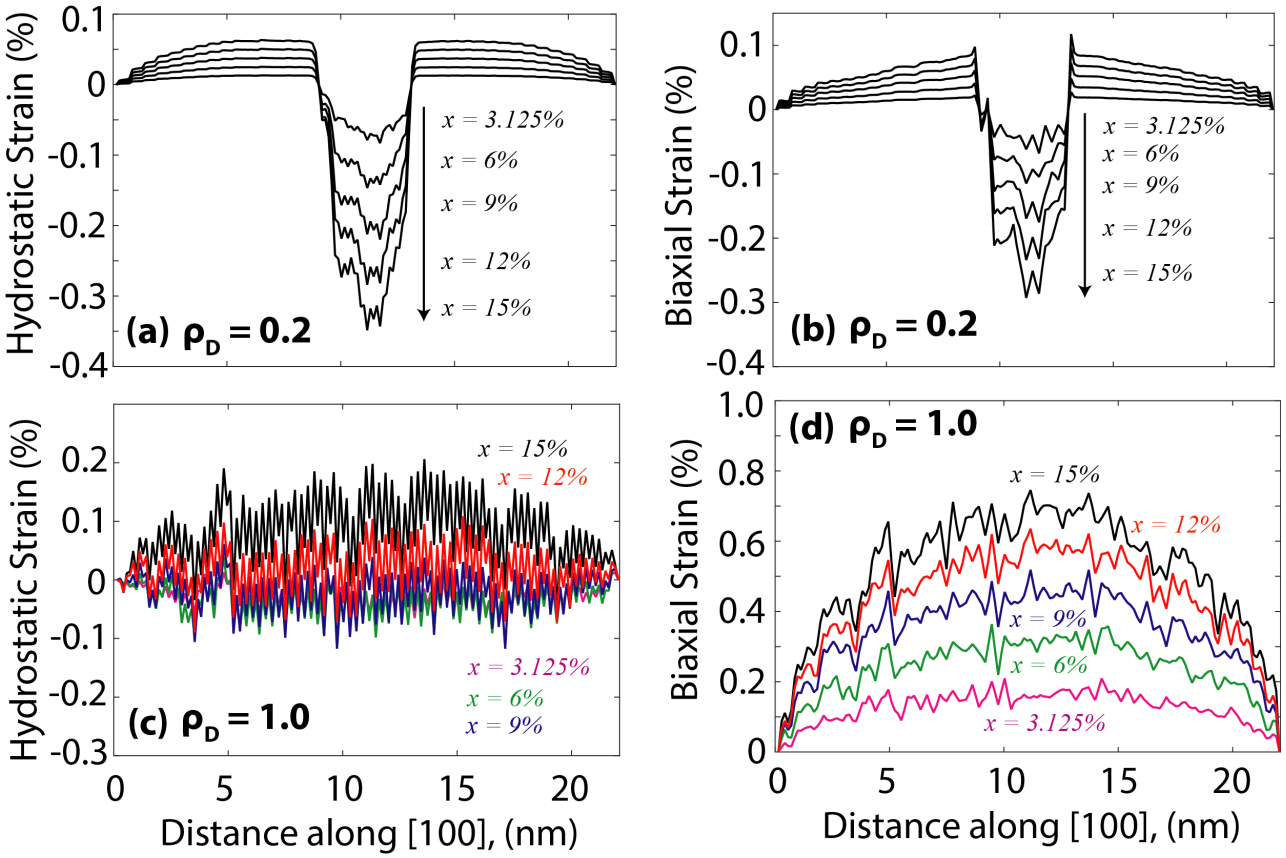

Supplementary Fig. S3. **(a,b)** The 1D plots of the hydrostatic and biaxial strain components are shown as a function of the Bi fraction (x) in the core region through the center of the nanowire with ρ_{D}=0.2. The computed strain at each data point along the [100] direction represents an average over all data points in the corresponding [100] plane and for five different random configurations of Bi atoms. **(c,d)** The same as **(a,b)** but for the nanowire structures with ρ_{D}=1.0.

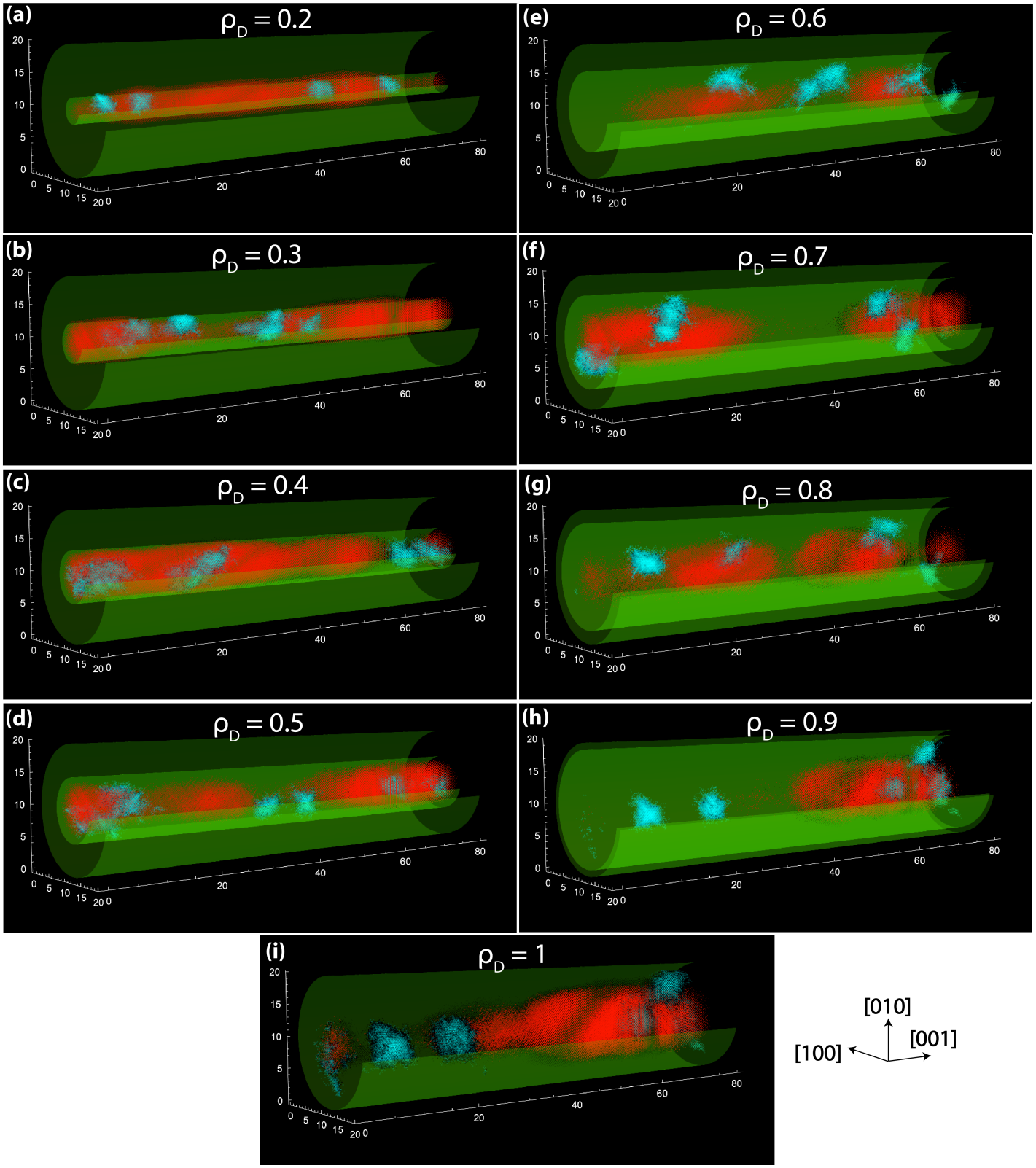

Supplementary Fig. S4. The three dimensional visualisations of charge densities are shown for the lowest electron (shown as red color distribution) and the highest hole (shown as cyan color distribution) states. The green cylinders are plotted to indicate the boundaries of the core and shell regions. The nanowires are selected with parameters as follows: D_S=20 nm, x=15%, ρ_L=4 and the values of ρ_D as marked on the plots.

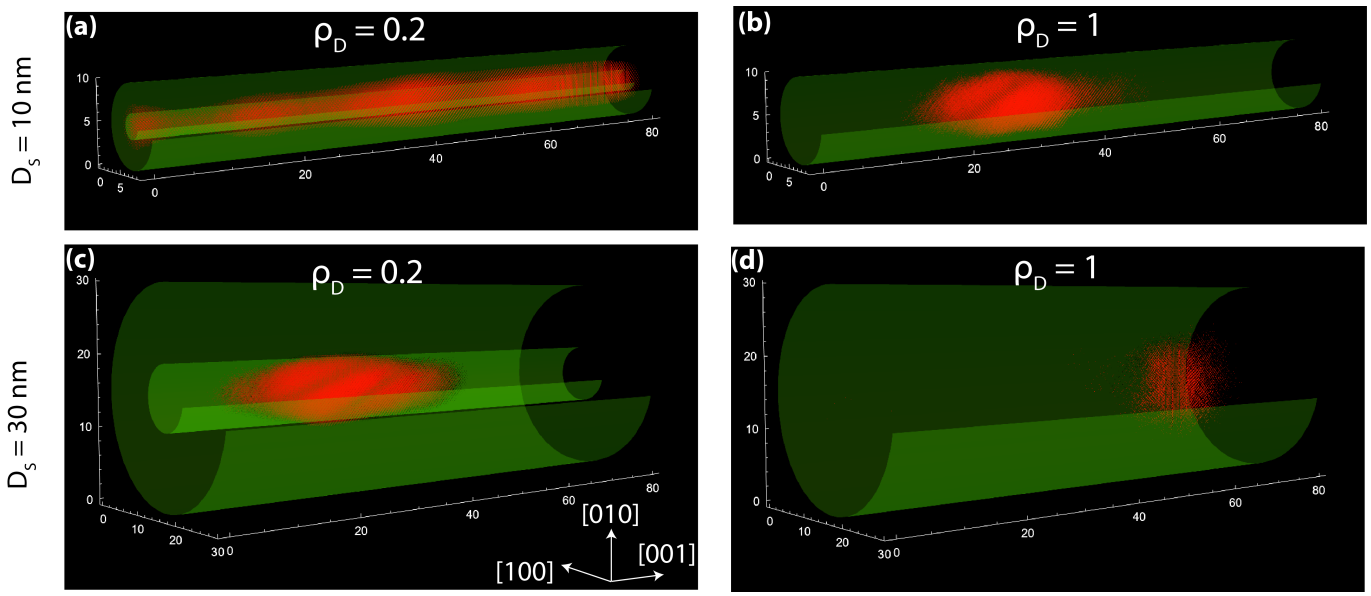

Supplementary Fig. S5. The three dimensional visualisations of charge densities are shown for the lowest electron (shown as red color distribution) and the highest hole (shown as cyan color distribution) states. The green cylinders are plotted to indicate the boundaries of the core and shell regions. The nanowires in (a,b) are selected with parameters as follows: D_S=10 nm, x=15% and ρ_L=4. The nanowires in (c,d) are selected with parameters as follows: D_S=30 nm, x=15% and ρ_L=4. The selected values of ρ_D are marked on the plots.

* musman@unimelb.edu.au

[1] Usman, M.; Broderick, C. A.; Batool, Z.; Hild, K.; Hosea, T. J. C.; Sweeney, S. J.; O'Reilly, E. P. Impact of alloy disorder on the band structure of compressively strained $GaBi_xAs_{1-x}$. *Phys. Rev. B* **2013**, *87*, 115104.

[2] Usman, M. Large-scale atomistic simulations demonstrate dominant alloy disorder effects in GaBiAs/GaAs multiple quantum wells. *Phys. Rev. Materials* **2018**, *2*, 044602.

[3] Keating, P. N. Effect of invariance requirements on the elastic strain energy of crystals with application to the diamond structure. *Phys. Rev.* **1966**, *145*, 637.

[4] Lazarenkova, O. L.; von Allmen, P.; Oyafuso, F.; Lee, S.; Klimeck, G. Effect of anharmonicity of the strain energy on band offsets in semiconductor nanostructures. *Appl. Phys. Lett.* **2004**, *85*, 4193.

[5] Usman, M.; Broderick, C. A.; Lindsay, A.; O'Reilly, E. P. Tight-binding analysis of the electronic structure of dilute bismide alloys of GaP and GaAs. *Phys. Rev. B* **2011**, *84*, 245202.

[6] Kent, P. R. C.; Zunger, A. Theory of electronic structure evolution in GaAsN and GaPN alloys. *Phys. Rev. B* **2001**, *64*, 115208.

[7] Usman, M.; Inoue, T.; Harda, Y.; Klimeck, G.; Kita, T. Experimental and atomistic theoretical study of degree of polarization from multilayer InAs/GaAs quantum dot stacks. *Phys. Rev. B* **2011**, *84*, 115321.

[8] Janotti, A.; Wei, S.-H.; Zhang, S. B. Theoretical study of the effects of isovalent coalloying of Bi and N in GaAs. *Phys. Rev. B* **2002**, *65*, 115203.

[9] Donmez, O.; Erol, A.; Arikan, M.; Makhloufi, H.; Arnoult, A.; Fontaine, C. *Semicond. Sci. Technol.* **2015**, *30*, 094016.

[10] Balanta, M. A. G.; Gordo, V. O.; Carvalho, A. R. H.; Puustinen, J.; Alghamdi, H. M.; Henini, M.; Galeti, H. V. A.; Guina, M.; Gobato, Y. G. Polarization resolved photoluminescence in GaAs1-xBix/GaAs quantum wells. *J. of Luminescence* **2017**, *182*, 49–52.

[11] Zhang, B.; Qiu, W.-Y.; Chen, P.-P.; Wang, X.-J. *J. Appl. Phys.* **2018**, *123*, 035702.

[12] Dybala, F.; Kopaczek, J.; Gladysiewicz, M.; Pavelescu, E.-M.; Romanitan, C.; Ligor, O.; Arnoult, A.; Fontaine, C.; Kudrawiec, R. *J. of Appl. Phys.* **2017**, *111*, 192104.

[13] Collar, K.; Li, J.; Jiao, W.; Guan, Y.; Losurdo, M.; Humlicek, J.; Brown, A. S. *AIP Advances* **2017**, *7*, 075016.

[14] Broderick, C. A.; Mazzucato, S.; Carrère, H.; Amand, T.; Makhloufi, H.; Arnoult, A.; Fontaine, C.; Donmez, O.; Erol, A.; Usman, M.; O'Reilly, E. P.; Marie, X. Anisotropic electron g factor as a probe of the electronic structure of $GaBi_xAs_{1-x}$/GaAs epilayers. *Phys. Rev. B* **2014**, *90*, 195301.

[15] Kudrawiec, R.; Kopaczek, J.; Polak, M.; Scharoch, P.; Gladysiewicz, M.; Misiewicz, J.; Richards, R.; Bastiman, F.; David, J. *J. Appl. Phys.* **2014**, *116*, 233508.

[16] Polak, M. P.; Scharoch, P.; Kudrawiec, R. *Semicond. Sci. Technol.* **2015**, *30*, 094001.

[17] Bannow, L. C.; Rubel, O.; Badescu, S.; Rosenow, P.; Hader, J.; Moloney, J.; Tonner, R.; Koch, S. *Phys. Rev. B* **2016**, *93*, 205202.

[18] Klimeck, G.; Ahmed, S. S.; Bae, H.; Kharche, N.; Rahman, R.; Clark, S.; Haley, B.; Lee, S.; Naumov, M.; Ryu, H.; Saied, F.; Prada, M.; Korkusinski, M.; Boykin, T. Atomistic simulation of realistically sized nanodevices using NEMO 3-D – part I: models and benchmarks. *IEEE Trans. Electron. Dev.* **2007**, *54*, 2079.

[19] Usman, M.; Bocquel, J.; Salfi, J.; Voisin, B.; Tankasala, A.; Rahman, R.; Simmons, M.; Rogge, S.; Hollenberg, L. *Nature Nanotechnology* **2016**, *11*, 763.

[20] Usman, M.; Tasco, V.; Todaro, M.; Giorgi, M.; O'Reilly, E.; Klimeck, G.; Passaseo, A. *Nanotechnology* **2012**, *23*, 165202.